MICROCOPY RESOLUTION TEST CHART

⑫

AD-A188 511

In-Situ Vibrational Spectroscopy of Specifically

Adsorbed Azide on Silver Electrodes

by

M. G. Samant
R. Viswanathan
H. Seki
P. S. Bagus
C. J. Nelin
M. R. Philpott

DTIC

SELECTE**D**

DEC 0 2 1987

D

Prepared for Publication

in

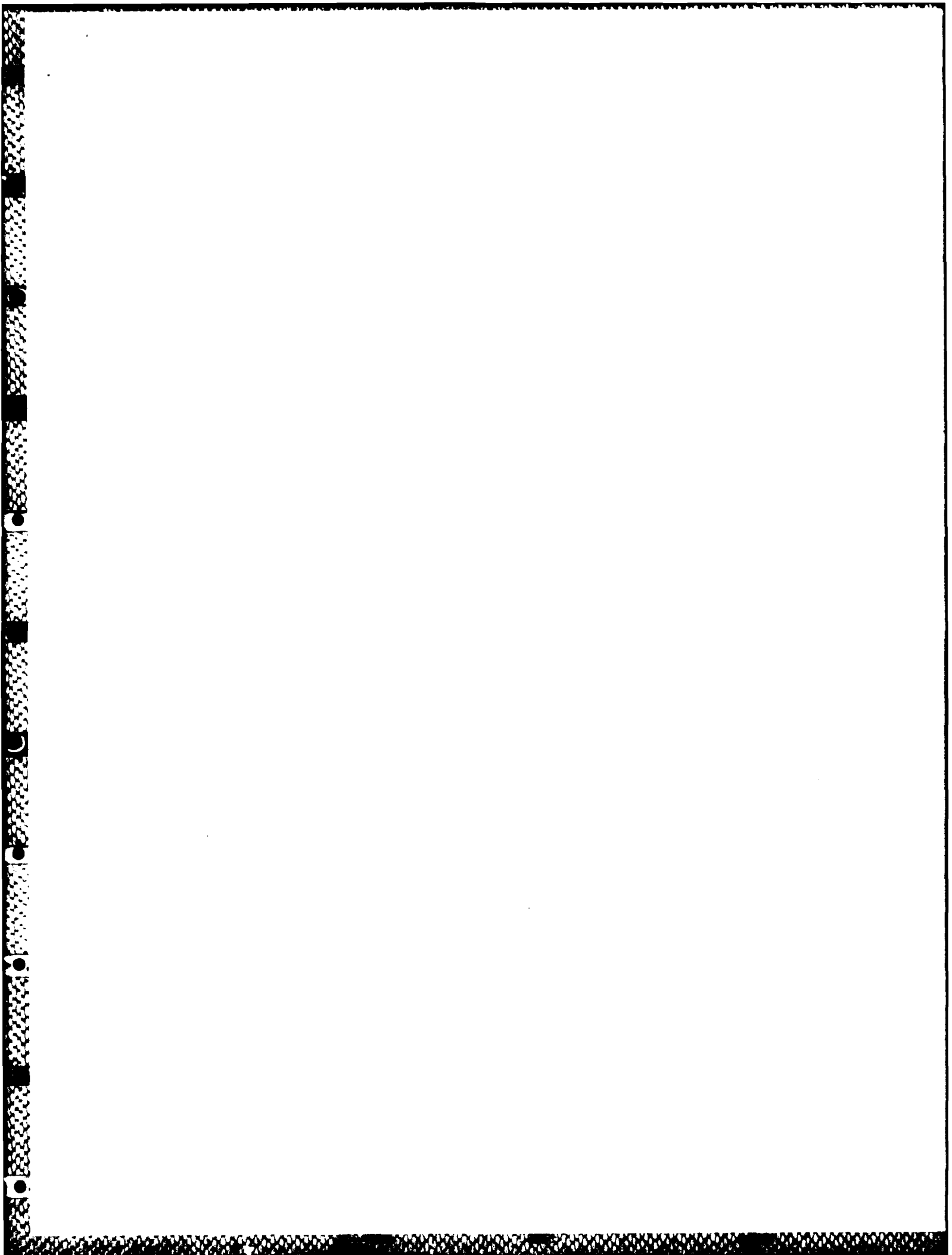*Journal of Chemical Physics*
(1987)

IBM Research

Almaden Research Center

650 Harry Road

San Jose, California 95120-6099

87 11 24 121

REPORT DOCUMENTATION PAGE		READ INSTRUCTIONS BEFORE COMPLETING FORM
1. REPORT NUMBER Technical Report No. 13	2. GOVT ACCESSION NO.	3. RECIPIENT'S CATALOG NUMBER
4. TITLE *(and Subtitle)* In-Situ Vibrational Spectroscopy of Specifically Adsorbed Azide on Silver Electrodes		5. TYPE OF REPORT & PERIOD COVERED Technical Report
		6. PERFORMING ORG. REPORT NUMBER
7. AUTHOR(s) M. G. Samant, R. Viswanathan, H. Seki, P.S. Bagus C. J. Nelin, M. R. Philpott		8. CONTRACT OR GRANT NUMBER(s) N00014-82-C-0583
9. PERFORMING ORGANIZATION NAME AND ADDRESS IBM Research Division, Almaden Research Center 650 Harry Road, San Jose, California 95120-6099		10. PROGRAM ELEMENT, PROJECT, TASK AREA & WORK UNIT NUMBERS
11. CONTROLLING OFFICE NAME AND ADDRESS		12. REPORT DATE November, 1987
		13. NUMBER OF PAGES 21
14. MONITORING AGENCY NAME & ADDRESS *(If different from Controlling Office)*		15. SECURITY CLASS *(of this report)* Unclassified
		15a. DECLASSIFICATION/DOWNGRADING SCHEDULE

16. DISTRIBUTION STATEMENT *(of this Report)*

Approved for public release: distribution unlimited.

17. DISTRIBUTION STATEMENT *(of the abstract entered in Block 20, if different from Report)*

Approved for public release: distribution unlimited.

18. SUPPLEMENTARY NOTES

19. KEY WORDS *(Continue on reverse side if necessary and identify by block number)*

infrared, vibrational spectroscopy, electrochemistry, silver, azide ⟵

20. ABSTRACT *(Continue on reverse side if necessary and identify by block number)*

In-situ infrared vibrational spectra of azide ions specifically adsorbed on polycrystalline silver electrodes immersed in aqueous electrolytes of composition 1 to 30 mM azide and 0.1M per-chlorate are reported for the potential range (I)0.25 to 0V *versus* Ag/AgCl (3M KCl). Adsorbed azide was not detected spectroscopically between 0V and -0.9V, a range (II) known from dif-ferential capacitance measurements to allow adsorption onto the silver electrodes. These

experimental observations have been interpreted with the help of *ab-initio* calculations of the vibrational frequencies of $[AgN_3]^0$ and $[AgN_3]^-$ for two configurations with $C_{\infty v}$ and C_{2v} symmetries representing primitive models for azide adsorbed with its configuration axis perpendicular and parallel to the electrode surface, respectively. Besides the charge states specified, calculations are also reported for statis applied fields along the symmetry axis. Taken together, the experiments and calculations support a model in which axide adsorbs oriented perpendicular to the surface at the higher surface concentrations induced by the more positive potentials of range I, and is adsorbed with long axis parallel to the surface in potential range II.

IN-SITU VIBRATIONAL SPECTROSCOPY OF SPECIFICALLY ADSORBED AZIDE ON SILVER ELECTRODES

M. G. Samant[*]
R. Viswanathan[*,+]
H. Seki
P. S. Bagus
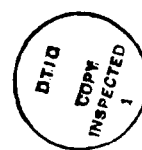C. J. Nelin[‡]
M. R. Philpott

IBM Research
Almaden Research Center
650 Harry Road
San Jose, California 95120-6099

ABSTRACT: In-situ infrared vibrational spectra of azide ions specifically adsorbed on polycrystalline silver electrodes immersed in aqueous electrolytes of composition 1 to 30 mM azide and 0.1 M perchlorate are reported for the potential range (I) 0.25 to 0V *versus* Ag/AgCl (3 M KCl). Adsorbed azide was not detected spectroscopically between 0V and −0.9V, a range (II) known from differential capacitance measurements to allow adsorption onto the silver electrodes. These experimental observations have been interpreted with the help of *ab-initio* calculations of the vibrational frequencies of $[AgN_3]^0$ and $[AgN_3]^-$ for two configurations with $C_{\infty v}$ and C_{2v} symmetries representing primitive models for azide adsorbed with its configuration axis perpendicular and parallel to the electrode surface, respectively. Besides the charge states specified, calculations are also reported for static applied fields along the symmetry axis. Taken together, the experiments and calculations support a model in which azide adsorbs oriented perpendicular to the surface at the higher surface concentrations induced by the more positive potentials of range I, and is adsorbed with long axis parallel to the surface in potential range II.

---

[*]IBM visiting scientist

[+]Permanent Address: Chemistry Department, Beloit College, Beloit, Wisconsin 53511.

[‡]Present Address: IBM Santa Teresa Laboratory, 555 Bailey Avenue, San Jose, California 95150

(M87J161)

I. INTRODUCTION

Specific adsorption of ions onto metal electrodes from stable double layers is believed to involve the squeezing out of solvent molecules from between the electrode surface and the ion so that they are in contact.[1] This phenomenon, which occurs from aqueous media for halides (except fluoride) and the pseudo-halides like CN^-, N_3^- and SCN^-, was originally postulated on the basis of differential capacitance measurements using a dropping mercury electrode.[2,3] Specific ion or contact ion adsorption, as it is also called, is believed to involve some degree of covalent bond formation between the ion and the electrode surface atoms with consequential partial discharge of the adsorbing ions. This partial discharge is described in terms of the electrosorption valence.[4-7] Direct contact adsorption of halides and pseudo-halides to noble metal electrodes is supported by the observation of the appropriate low frequency metal-ligand stretching modes seen in surface enhanced raman spectra (SERS) of roughened electrodes,[8] and by the observation of the internal stretching modes of cyanide (CN^-)[9-12] and thiocyanate (SCN^-)[13,14] adsorbed on unroughened (i.e., polished) electrodes by in-situ fourier transform infrared (FTIR) spectroscopy.

In this paper, we consider azide (N_3^-) adsorbed on unroughened polycrystalline silver electrodes in azide solutions with 0.1M sodium perchlorate as supporting electrolyte. All reported potentials are measured relative to the Ag/AgCl (3M KCl) reference electrode. The SERS of azide on silver shows some anomalies not exhibited by cyanide or thiocyanate[15]. In particular, for 50 mM azide, the raman signals at 1334 cm^{-1} were stable at potential more positive than 0.17V (Ag/AgCl) and decaying between 0 and 0.17V (Ag/AgCl). They were not seen at potential less than 0.0V. Differential capacitance measurements[16,17] and recently both SERS and potential difference infrared (PDIR) measurements[18,19] indicate the existence of adsorbed azide throughout the entire double layer potential range between $-0.9V$ and 0.25V, Ag/AgCl. This is consistent with measurements of azide adsorption on mercury.[20,21] We use polarization modulated Fourier transform infrared reflection absorption spectroscopy

(PM-FT-IRRAS)[22] to measure directly the asymmetrical stretch of adsorbed azide near 2080 cm^{-1}. This band is potential dependent and is distinguished thereby from the solution species which has an infra red active frequency v_{as} at 2050 cm^{-1}.

Ab-initio self-consistent field (SCF) wavefunctions have been obtained for a simple cluster chosen to model the consequences of the metal-azide interaction. The cluster used is $[AgN_3]^{0,-}$ and two geometries are considered. In the first geometry, the Ag atom and the (linear) N_3 molecule are colinear; this models N_3 adsorption at an on-top Ag site where the N_3 molecular axis is oriented normal to the surface. In the second geometry, the Ag atom is located directly beneath the central N atom to model N_3 adsorption in a parallel orientation. The point group symmetries for these two geometries is $C_{\infty v}$ for the colinear AgN_3 and C_{2v} for the parallel orientation. Two total charges for the cluster, $[AgN_3]^0$ and $[AgN_3]^-$, are also considered to model two effects. The first is a very simple representation of the effect of the other silver atoms of the electrode and the second is electrode charging as the applied potential is made negative. This theoretical study has provided essential insights into the behavior of the Ag-N_3 and N_3 vibrational modes. Calculations are reported for the low frequency metal-ligand mode v_{ML}, ligand symmetrical stretch v_s (1340 cm^{-1} raman active) and for the ligand asymmetrical stretch v_{as} (2050 cm^{-1} infrared active); no calculations for the angle bend mode v_δ (640 cm^{-1} infrared active) are reported here. The shift in the vibrational modes for static electric fields of strength $\pm 5.2 \times 10^7$ V/cm are also reported since, together with the influence of total charge state (0 or -1), these calculations show the likely dependence of vibrational frequency on the electric field in the compact part of the double layer. The small AgN_3 cluster and the uncorrelated SCF wave functions will not give precise quantitative values[23] for v_{ML}, v_s and v_{as} for adsorbed N_3. However, our objective is to identify trends and changes in the values which are relevant to the surface, and to identify the mechanisms responsible for these trends. In particular, we show that the theoretical evidence strongly supports a simple physical model for the origin of the electric field induced shifts of v_{as} for azide adsorbed in the perpendicular orientation as

N_3^-. The shifts arise because the electric fields induce large changes in the metal-ligand bond distances and the vibrational frequency depends strongly on the distance of the ligand from the "wall" of surface charge.[23]

All the evidence taken together consistently supports a model in which azide is ionically bound to the electrode at all double layer potentials, being oriented parallel in the range $-0.9V$ to ca. 0.0V and perpendicular in the range ca. 0.0V to 0.25V. Corrigan et al[18,19] have suggested the same model based on raman and potential modulated FTIR data.

II. VIBRATIONAL SPECTRA OF AZIDE IONS

The isolated azide ion has $D_{\infty h}$ symmetry, and therefore, its vibrational modes are either infrared or raman active. In aqueous solutions, the fundamental modes are: ν_δ (ca. 640 cm^{-1}), a twofold degenerate angle bending mode, ir allowed; ν_s (ca. 1340 cm^{-1}) symmetric stretch, raman active; ν_{as} (ca. 2050 cm^{-1}), asymmetric stretch, ir active. In addition, a Fermi resonance occurs between $2\nu_\delta$ and ν_s, and the vibrations $3\nu_\delta$ and $\nu_s + \nu_\delta$ fall near ν_{as}, providing additional sources of fine structure in solution and solid state spectra.

Figure 1 shows schematically the symmetrical and asymmetrical modes as well as the metal-ligand stretch for parallel and perpendicular orientations of an azide anion over a flat surface. The top site silver atom is shown shaded, and this is the only surface atom considered in the SCF calculations described below. Nitrogen atoms of the azide ion are labelled N1, N2 and N3, the unlabelled circles represent the surface Ag atom, with the top-site atom shaded as mentioned previously. The ir and vibrational raman spectra of alkali metal azides[24,25] and silver azide[26] have been well studied.

III. EXPERIMENTAL FT-IRRAS VIBRATIONAL SPECTRA

The infrared measurements were made in reflection geometry using an IBM IR/98 Fourier transform spectrometer. Details of the construction of the electrochemical cell and the polarization modulation IRRAS technique used and developed by us are available elsewhere.[27] A liquid nitrogen cooled InSb detector (Infrared Associates) was used. The incident light was modulated by a photoelastic modulator system (Hinds International) with a frequency setting of 2150 cm^{-1}. Under these conditions the lower detection limit was 1800 cm^{-1}. A lock-in amplifier (PAR) was used to obtain the intensity difference of the spectrum obtained with s and p polarized light, I(s)-I(p). The spectra presented here are the ratio [I(s)-I(p)]/[I(s)+I(p)] and represent an average of 300 scans each of about two seconds duration.

The electrolytes were prepared from reagent grade NaN_3 and $NaClO_4$ which were further purified by recrystallization. The water used was first deionized and rendered organic-free by a Barnsted "Nanopure" system with an "Organopure" attachment. The solutions examined had azide concentrations of 1, 3, 10 and 30 mM in 0.1M sodium perchlorate. The silver electrode was prepared by mechanically polishing it sequentially with 5, 1.0 and 0.3 micron alumina on a pad using water as a lubricant. The electrode was then ultrasonically cleaned and repeatedly electrochemically cycled. The electrolyte in the infrared cell was deaerated by bubbling nitrogen gas before the experiment.

For the spectra presented here the electrode was pulled back approximately 0.5 cm from the window before altering the potential, so that equilibrium with the bulk solution was established during the change. Then the electrode was returned accurately to its former position using a micrometer movement. This is an experimental procedure which differs with that of Corrigan et al.[18,19] Using this procedure it is possible to obtain spectra that are reversible with potential so long as the potential is kept within the double layer region. Note that at a few mM azide concentration there is only approximately the equivalent of a monolayer of azide in solution in front of the electrode

when the electrode is pressed against the window (assuming a solution thickness of a few microns).

Figure 2 shows a set of spectra in the range of 1980 cm^{-1} and 2120 cm^{-1} from a 30 mM azide solution, recorded at different potentials. The spectrum of an azide free solution was used to subtract out the background in these spectra. Figure 3 shows the same set of spectral data but with the azide spectrum at $-0.9V$ subtracted. In Figure 2 the azide solution band at 2050 cm^{-1} dominates. Note that at more positive potentials, a shoulder appears at approximately 2100 cm^{-1}. The true nature of this shoulder is revealed in Figure 3 which shows that the strong 2050 cm^{-1} solution absorption hides a potential dependent surface azide band which appears first at 2070 cm^{-1} (0.1V) and advances to ca. 2085 cm^{-1} (0.25V) as the potential is made more positive. Figure 4 shows the positions of the surface azide vibrational frequency (cm^{-1}) plotted against electrode potential. The slope is approximately 100 cm^{-1}/V if one assumes a linear dependence of the frequency on the potential.

IV. CALCULATED VIBRATIONAL FREQUENCIES

The experimental vibrational spectra reported in the last section show that surface adsorbed azide has a vibrational frequency at higher energy than in solution and that as the electrode is made more positive, this frequency shifts to even higher energy. To test the plausibility of this explanation, we have calculated the three vibrational modes of the neutral $[AgN_3]^0$, and ion $[AgN_3]^-$ for the azide moiety in end on $(C_{\infty v})$ and flat (C_{2v}) configurations. The three modes and two configurations are essentially those shown in Figure 1 when the unshaded surface Ag atoms are ignored. Analysis of the AgN_3 cluster charge density showed that the azide ligand occurred always as the N_3^- anion. This is true for both the neutral $[AgN_3]^0$, and charged $[AgN_3]^-$ clusters and for both colinear $(C_{\infty v})$ and parallel (C_{2v}) cluster geometries. Qualitatively, this is the same as we found for the cyanide ligand on copper clusters representing the (100) face.[28]

Based on previous experience using metal atom clusters of various sizes to represent metal surfaces we expect the vibrational results for the neutral and anion silver azide molecule to bracket those for a large cluster or for an extended surface. This follows from the ionic character of the adsorbed azide which is best visualized as N_3^-. The metal will polarize in response to the presence of N_3^-; this is often described as forming an image charge in the metal. For $[AgN_3]^0$, the charge needed to form N_3^- comes entirely from the single Ag atom and the electrostatic interaction between a polarized surface and adsorbed azide is an overestimate of the interaction between a polarized surface and adsorbed N_3. For $[AgN_3]^-$, the charge needed to form N_3^- is supplied externally. While the single Ag atom is able to polarize to some extent in response to the presence of N_3^-, this polarization is much smaller than for larger clusters or for an extended surface.[29] Thus, the interaction in $[AgN_3]^-$ is an underestimate of the Ag ... N_3 surface interaction. We do not expect either $[AgN_3]^0$ or $[AgN_3]^-$, to fully reproduce the situation at the electrode surface. However, when we find common behavior in the electric field induced changes of the vibrational frequencies for $[AgN_3]^0$

and $[AgN_3]^-$, we expect this behavior to apply at the surface. This is the spirit in which the calculations were performed.

We have carried out SCF calculations for various interatomic distances and used the resulting potential surfaces to obtain the vibrational frequencies. Note that the calculations have been carried out in the absence of an applied electric field, ($F = 0$ case), and in a static uniform electric field of $F = \pm 0.01$ a.u. $= \pm 5.2 \times 10^7$ V cm normal to the surface. This field is typical of those existing inside the compact part of the Helmholtz double layer. Details of how the computations are carried out are described elsewhere.[23,28,29] In order to describe the bond distance variation, we denote the azide atoms as N1, N2 and N3 where N2 is the central atom of linear N_3. For the colinear $C_{\infty v}$ geometry N1 is closest to Ag while for the parallel C_{2v} geometry, N2 is closest to Ag; see Figure 1. We first held $r(N1-N2) = r(N2-N3) = 2.22$ bohrs, the equilibrium value for free N_3^-, and varied the Ag-N_3 distance. This was done for $F = 0$ and ± 0.01 a.u. and for both $C_{\infty v}$ and C_{2v} geometries. From this variation, we obtained equilibrium distances and metal-ligand frequencies ν_{ML}, where the Ag mass was assumed infinite. We then fixed $r(Ag-N2)$, as appropriate for the geometry and field, and varied $r(N1-N2)$ and $r(N2-N3)$ independently to obtain ligand equilibrium distances and stretching frequencies ν_s and ν_{as}. This procedure neglects the coupling between ν_{ML}, and the two intra ionic frequencies ν_s and ν_{as}. However, since ν_{ML} is much smaller than either ν_s or ν_{as}, the coupling should be very small and this neglect is not expected to be significant.[23] Note that our procedure has taken the coupling of ν_s and ν_{as} fully into account. We have also computed the vibrational frequencies for free N_3^-. For $F = \pm 0.01$ a.u., the same constraint for N_3^-, as for AgN_3 was applied; namely the position of the N2 nitrogen atom was fixed and the positions of atoms N1 and N3 were varied. The purpose of the free N_3^- calculations was to provide direct information for comparison about the influence of the presence and absence of Ag on ν_s and ν_{as}. The results of the *ab-initio* calculations are summarized in Tables I and II.

V. DISCUSSION

The experimental IRRAS spectra can be interpreted assuming that there are two orientations for adsorbed azide. When the azide is adsorbed in the flat configuration, the complex $[AgN_3]^{0,-}$ has a C_{2v} point group. The modes v_{ML}, $v_\delta(z)$ and v_s have A_1 symmetry and the modes v_{as} and $v_\delta(y)$ have B_1 and B_2 symmetry, respectively. The intensity of the ir transition to the symmetrical stretch v_s is expected to be very weak. However, coupling among the three A_1 modes should result in intensity transfer from the modes with higher intensity v_{ML} and $v_\delta(z)$ to the weaker v_s mode. The other two modes, $v_\delta(y)$ and v_{as}, having B symmetry are not mixed either together or to the totally symmetrical models and, therefore, remain dipole forbidden. These arguments based on symmetry hold in the presence of the externally applied static field with direction parallel to z.

When azide adsorbs axial, the complex AgN_3 representing the adsorption site has $C_{\infty v}$ symmetry. Now v_{ML}, v_s and v_{as} are all A modes and, therefore, mix under the action of totally symmetric perturbations like the axial electric field. We expect v_{ML} and v_{as} to be strongest according to the surface selection rule. The symmetric mode v_s which in the absence of Ag has no dipole intensity will couple to the other two modes and borrow intensity. The angle bend modes v_δ have higher symmetry and neither mix or become dipole allowed through couplings to the optical modes v_{ML} and v_{as}. Anharmonicities within the ion, or induced by fields or interactions with surface atoms will induce mixing of v_{ML} and v_δ with each other and v_s making the latter weakly allowed. Also, the Fermi resonance between $2v_\delta$ and v_s will be very weakly allowed, as will the overtone and combinations $3v_\delta$ and $v_\delta + v_s$ which fall in the region of v_{as}.

The calculations for 'flat' adsorbed azide (see $[AgN_3]^0$ and $[AgN_3]^-$ with C_{2v} symmetry in Tables I and II) support the hypothesis of two orientations of the adsorbed azide in the following way. First, we note that the internal geometry of the ion is essentially unchanged at 2.22 bohr for all fields ($F = 0, \pm 0.01$) and charge states $(0, -1)$. There is a strong field dependence in v_{ML} and the Ag-N2 distance for both charge states

$(0, -1)$, with the $[AgN_3]^-$ showing the greatest dependence because of the absence of monopole electrostatic interaction between Ag^0 and N_3^-. The effect of the charge of the silver atom and the field F on the raman mode v_s is weak since it is only slightly red shifted from the isolated ion value of 1411 cm^{-1}. In contrast, the effects of the charge of the silver atom and field F is stronger for the asymmetrical stretching mode v_{as}. As with the raman mode v_s, there is a shift to lower frequency which is understandably greatest for $[AgN_3]^0$ because of the strong coulombic field of the silver ion Ag^+. As the N_3^- moves away from the silver ion, note how quickly the ir mode v_{as} approaches the isolated N_3^- value. We note, see Table I, that for free N_3^- the electric field does not change v_s and v_{as} for the orientation N_3 parallel to the surface. This is entirely expected since N_3 does not have a dipole moment in the direction of the field; hence, it does not interact with the field. It is reasonable that the field induced shifts in v_s and v_{as} for AgN_3 with C_{2v} geometry are due to the interaction between Ag and N_3. This is likely to arise from the polarization of the N_3^- charge by the Ag atom. This polarization changes the v_s and v_{as} differently for $F = 0, 0.01$ and -0.01 a.u. (We have noted a similar effect for cluster calculations that model the two perpendicular orientations of CN on a Cu(100) surface, namely CN with N down and CN with C down.[31])

Consequently, the calculations predict that for azide adsorbed flat, the stretching modes are shifted to lower energy, below the 2050 cm^{-1} solution peak in the case of v_{as}. Further, we predict strong field dependence on v_{ML} and, by inference, v_δ. Any field induced intensity in the IRRAS spectra are predicted to appear in the low frequency tail of the 2050 cm^{-1} solution band of the azide ion. Detector sensitivity and polarization modulator absorption of ir light prevent us from exploring the 640 cm^{-1} region of the v_δ mode with our current FTIR spectrometer.

Our calculations also predict that azide adsorbed on silver surfaces with the central nitrogen N2 at an on-top site will be further from the surface than when adsorbed perpendicularly as through nitrogen N1. In both cases the azide will also be ionic and not covalently bonded. Although the center of charge is on N2 the ion has charge

almost equally on the terminal and central atoms and there is a strong axial quadrupole. In two dimensions, axial quadrupoles orientate in a T-bone lattice. Consequently, at low coverages, azide may adsorb as islands with a T-bone lattice arrangement.

In the range (I), 0 to 0.25V, it is postulated that azide adsorbs mainly end on *via* nitrogen N1 to the metal surface. The calculations shown in Tables I and II support the interpretation. Both stretching modes v_{as} and v_s are shifted to higher frequencies. The effect is greatest for v_{as} which shows both charge and field effects. A comparison of the v_{as} and v_s calculated for free N_3^- and $[AgN_3]^0$ in $C_{\infty v}$ geometry indicate the origin of these field induced shifts. Note that for the free azide anion with F parallel to N_3^- the shift in v_{as} is small, $\simeq 16 cm^{-1}$, and to a higher frequency. (The shifts for free N_3^- are the same, as they should be, for $F = \pm 0.01$.) The shifts are much larger for $[AgN_3]^0$ and $[AgN_3]^-$, increasing for $F = -0.01$ and decreasing for $F = 0.01$ a.u. The applied electric field also leads to large changes for the metal-azide distance, smaller for $F = -0.01$ and larger for $F = 0.01$. This is to be expected: the field exerts a strong force on the adsorbed azide since it is ionic.

It has been shown for CN/Cu(100) that the CN stretch frequency depends strongly on the distance of the CN from the metal surface.[23] When CN is closer to the surface, the frequency is larger and when CN is further from the surface, the frequency v_{CN} is smaller. This is closely related to the nonbonding overlap of the ligand and metal surface charge.[31] This overlap makes a repulsive contribution to the interaction and leads to an increase in v. When the ligand is closer to the surface, the increase is larger and when it is further away, the increase is smaller. This explanation is entirely consistent with our azide results for v_{as}. It is surprising that this nonbonding overlap effect does not also lead to large field induced shifts for v_s. These are calculated for AgN_3^- ($C_{\infty v}$) to be an order of magnitude smaller than the shifts in v_{as}. However, note that the shifts of v_s for free N_3^- are $\simeq 30 cm^{-1}$ to lower frequency while the shifts due to the nonbonding overlap are to higher frequency. It is possible that these shifts cancel; further calculations are required to investigate this possibility. The decrease in the

N1-N2 bond distance is almost 0.1 bohr for $[AgN_3]^0$ in the field $F = -0.01$ which pulls

the ligand toward the Ag^+ ion, thereby enhancing its polarization of the anion and

stabilizing the $(N1 \equiv N2-N3)^-$ over the $(N1-N2 \equiv N3)^-$ mesomeric form. The

experimental shift for v_{as} was approximately 30 cm^{-1} from solution to surface

adsorption (Section II), which is much smaller than the minimum shift we calculate of

approximately 120 cm^{-1} (AgN_3^- in $F = 0.0$). However, this comparison is not quite

right since we are subtracting a solution shifted value of 2050 cm^{-1}. It has been

estimated that vacuum azide has $v_{as} \simeq 2007 \text{ cm}^{-1}$ so that the corrected experimental shift

to be compared to the calculated vacuum value would be approximately 80 cm^{-1}. This

neglects the solvent shift of the adsorbed azide and though it compares more favorably

with the calculated values, it is undoubtedly too large. The danger here is to

overinterpret the theoretical calculations. The important point is the qualitative

agreement between theory and experiment.

VI. SUMMARY AND CONCLUSION

Theoretical *ab-initio* calculations of the ν_{ML}, ν_s and ν_{as} vibrational modes of $[AgN_3]^0$ and $[AgN_3]^-$, for $C_{\infty v}$ and C_{2v} geometries, assuming that the silver nucleus is fixed, have been used to support the interpretation of the IRRAS spectra of azide adsorbed on polycrystalline Ag electrodes in the Helmholtz double layer range of potentials. Our discussion has neglected lateral interactions as a source of frequency shift with potential. In the case of perpendicular orientation, direct through space, vibrational exciton coupling will also give a shift to higher frequencies with increasing coverage. By inference, we have also suggested that ν_{ML} and one ν_δ mode will be strongly coupled together and to the stretching mode for flat adsorption and to both modes ν_s and ν_{as} for axial ($\|z$) adsorption. For the more anodic double layer potentials, azide is preferentially adsorbed perpendicular to the surface and the ir mode ν_{as} shifts to higher frequencies at increasingly anodic potentials. In contrast, the raman mode ν_s is only weakly dependent on field for both orientations. SERS of 50 mM azide in contact with Ag showed no potential dependence of the ν_{as} mode,[14] in agreement with the calculations.

We believe through the work described here that use of ir spectroscopy in conjunction with cluster-adsorbate calculations is a potent tool in the study of complex interfaces such as those found in electrochemical double layers.

ACKNOWLEDGMENT

TABLE I

Summary of Internal Geometry and the High Frequency Stretching Modes
for Isolated N_3, $[AgN_3]^0$ and $[AgN_3]^-$
in Applied Static Electric Fields $F = 0, \pm 0.01$.[a]

System[b]	Field F a.u.[a]	r(N1-N2) bohr[a]	r(N2-N3) bohr[a]	ν_{as} cm^{-1}	ν_s cm^{-1}
$N_3^- \parallel F$	−0.01	2.19	2.26	2012	1384
$C_{\infty v}$	0	2.22	2.22	1996	1411
	+0.01	2.26	2.19	2012	1384
$N_3^- \perp F$	−0.01	2.22	2.22	1997	1411
C_{2v}	0	2.22	2.22	1996	1411
	+0.01	2.22	2.22	1997	1411
$[AgN_3]^0$	−0.01	2.13	2.28	2286	1507
$C_{\infty v}$	0	2.16	2.26	2216	1501
	+0.01	2.18	2.23	2160	1493
$[AgN_3]^-$	−0.01	2.15	2.26	2205	1488
$C_{\infty v}$	0	2.18	2.23	2119	1483
	+0.01[b]	--	--	--	--
$[AgN_3]^0$	−0.01	2.23	2.23	1839	1379
C_{2v}	0	2.23	2.23	1908	1384
	+0.01	2.23	2.23	1949	1393
$[AgN_3]^-$	−0.01	2.22	2.22	1933	1396
C_{2v}	0	2.22	2.22	1969	1408
	+0.01[c]	--	--	--	--

[a]For fields 0.01 a.u. = 5.2×10^7 V/cm, for geometries 1 bohr = 0.529Å.

[b]Notation $C_{\infty v}$ means azide is adsorbed N1 nitrogen down with its long axis perpendicular to the surface. Notation C_{2v} means azide is adsorbed parallel to the surface.
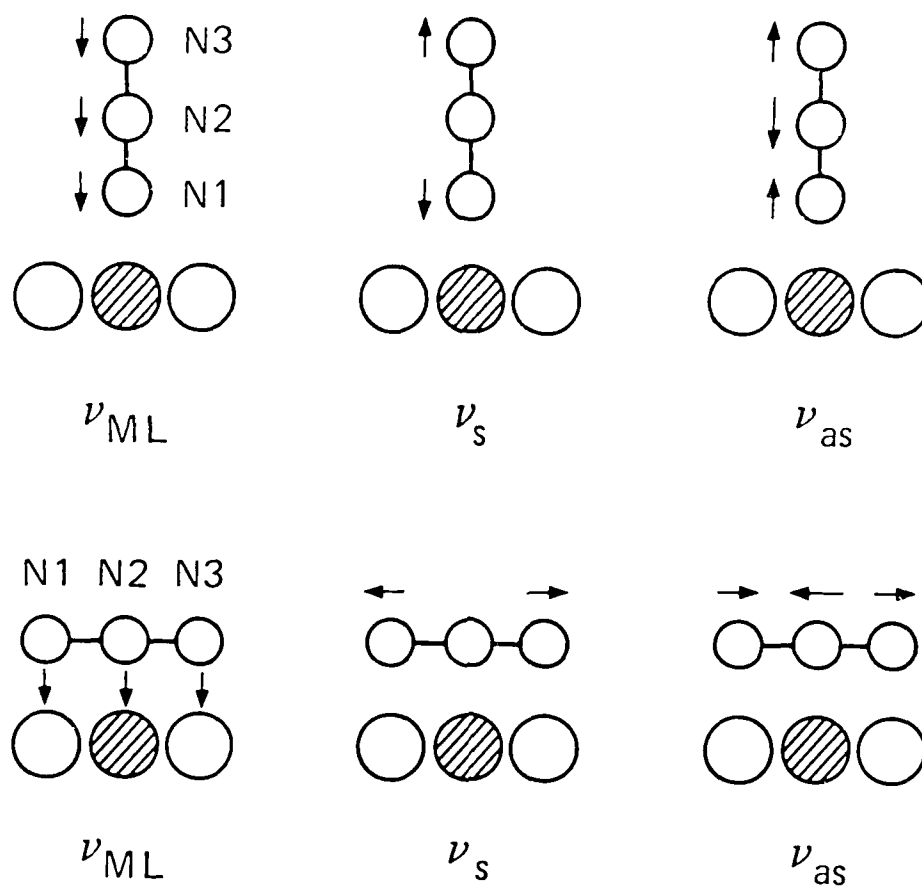
[c]This geometry not stable in a repulsive electric field of $F = +0.01$.

TABLE II

Summary of Geometry and Low Frequency Metal-Ligand Stretching Mode for $[AgN_3]^0$ and $[AgN_3]^-$ in Applied Static Electric Fields $F = 0, \pm 0.01$.[a]

System[b]	Field F a.u.[a]	r(Ag-N1 or N2)[c] bohr[a]	ν_{ML} cm^{-1}
$[AgN_3]^0$ $C_{\infty v}$	−0.01	3.87	305
	0	3.97	269
	+0.01	4.11	221
$[AgN_3]^-$ $C_{\infty v}$	−0.01	4.07	237
	0	4.34	165
	+0.01[d]	--	--
$[AgN_3]^0$ C_{2v}	−0.01	4.46	226
	0	4.43	189
	+0.01	4.91	140
$[AgN_3]^-$ C_{2v}	−0.01	4.84	158
	0	5.49	84
	+0.01[b]	--	--

[a]For fields 0.01 a.u. $= 5.2\times10^7$ V cm, for geometries 1 bohr $= 0.529$Å.

[b]Notation $C_{\infty v}$ means azide is adsorbed N1 nitrogen down with its long axis perpendicular to the surface. Notation C_{2v} means azide is adsorbed parallel to the surface.

[c]The distance r(Ag-N1 or N2), see Fig. 1, denotes distance from the shaded Ag to nearest nitrogen N1 for $C_{\infty v}$ or C_{2v}.

[d]This geometry not stable in a repulsive electric field of $F = 0.01$.
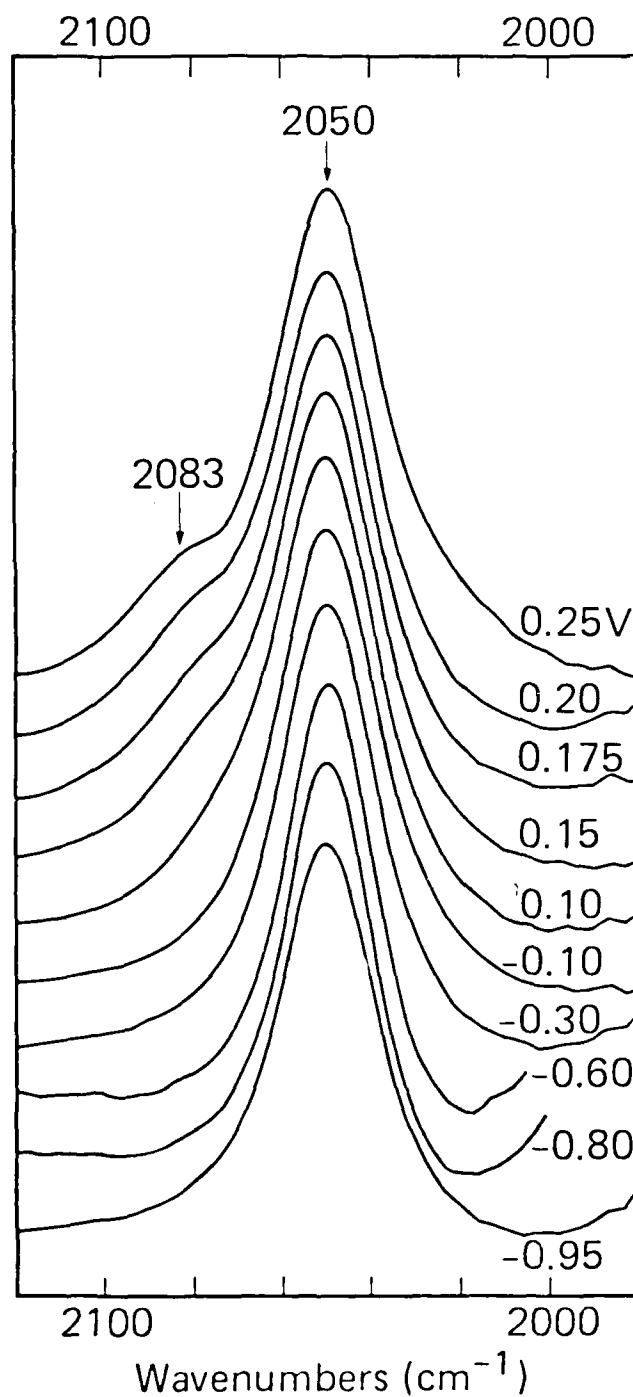
REFERENCES

1. M. A. Habib and J. O'. M. Bockris, in *Comprehensive Treatise of Electrochemistry*, Vol. 1, edited by J. O' M. Bockris, B. E. Conway and E. Yeager (Plenum Press, New York, 1980), Chap. 4.

2. D. C. Grahame, *J. Amer. Chem. Soc.* **80**, 4201 (1958).

3. D. C. Grahame and R. Parsons, *J. Amer. Chem. Soc.* **83**, 1291 (1961).

4. J. W. Schultze and K. J. Vetter, *Electroanalytical Chemistry & Interfacial Electrochemistry* **44**, 63-81 (1973).

5. J. W. Schultze and F. D. Koppitz, *Electrochimica Acta* **21**, 327-336 (1976).

6. F. D. Koppitz and J. W. Schultze, *Electrochimica Acta* **21**, 337-343 (1976).

7. D. M. Kolb, *Advances in Electrochemistry & Electrochemical Engineering*, edited by H. Gerischer and C. W. Tobias, **11**, 125-271 (1978).

8. See, for example: P. Gao and M. J. Weaver, *J. Phys. Chem.* **90**, 4057-4063 (1986).

9. K. Kunimatsu, H. Seki and W. G. Golden, *Chem. Phys. Lett.* **108**, 195-199 (1984).

10. K. A. Bunding Lee, K. Kunimatsu, J. G. Gordon, W. G. Golden and H. Seki, *J. Electrochem. Soc.* **134**, 1676-1678 (1987).

11. K. Kunimatsu, H. Seki, W. G. Golden, J. G. Gorden and M. R. Philpott, *Surface Sci.* **158**, 596-608 (1985).

12. K. Kunimatsu, H. Seki, W. G. Golden, J. G. Golden and M. R. Philpott, *Langmuir*, submitted.

13. J. K. Foley, S. Pons and J. J. Smith, *Langmuir* **1**, 697-701 (1985).

14. D. S. Corrigan, J. K. Foley, P. Gao, S. Pons and M. J. Weaver, *Langmuir* **1**, 616-620 (1985).

15. R. E. Kunz, J. G. Gordon II, M. R. Philpott and A. Girlando, *J. Electroanal. Chem.* **112**, 391-395 (1980).

16. D. Larkin, K. L. Guyer, J. T. Hupp and M. J. Weaver, *J. ELectroanal. Chem.* **138**, 401 (1982).

17. J. T. Hupp, D. Larkin and M. J. Weaver, *Surf. Sci.* **125**, 429 (1983).

18. Dennis S. Corrigan and M. J. Weaver, *J. Phys. Chem.* **90**, 5300-5306 (1986).

19. D. S. Corrigan, P. Gao, L. H. Leung and M. J. Weaver, *Langmuir* **2**, 744-752 (1986).

20. C. V. D'Alkaine, E. G. González and R. Parsons, *J. Electroanal. Chem.* **32**, 57 (1971).

21. E. R. González, *J. Electroanal. Chem.* **90**, 431-438 (1978).

22. W. G. Golden and D. Sapperstein, *J. Electron Spectroscopy and Related Phenomena* **30**, 43 (1983).

23. see P. S. Bagus, C. J. Nelin, K. Hermann and M. R. Philpott, *Phys. Rev. B*, submitted and references therein.

24. R. T. Lamoureux and D. A. Dows, *Spectrochimica Acta* **31A**, 1945-1949 (1975).

25. J. I. Bryant and G. C. Turrell, *J. Chem. Phys.* **37**, 1069-1077 (1962).

26. J. I. Bryant and R. L. Brooks, *J. Chem. Phys.* **54**, 5315-5323 (1971).

27. H. Seki, K. Kunimatsu, W. G. Golden, *Appl. Spectrosc.* **39**, 435-443 (1985).

28. P. S. Bagus, C. J. Nelin, W. Müller, M. R. Philpott and H. Seki, *Phys. Rev. Lett.* **58**, 559 (1987).

29. P. S. Bagus, K. Hermann, Ph. Avouris, A. R. Rossi and K. C. Prince, *Chem. Phys. Lett.* **118**, 311 (1985).

30. N. A. Shumilova and G. V. Zhutaeva, in *Encylopedia of Electrochemistry of the Elements*, vol 8, edited by A. J. Bard, Marcel Dekker, N. Y. (1978).

31. C. J. Nelin, P. S. Bagus and M. R. Philpott, *J. Chem. Phys.* **00**, 0000 (1987).

32. P. S. Bagus and W. Müller, *Chem. Phys. Lett.* **115**, 540 (1985).

Figure 1. Schematic diagram showing the relation of metal-ligand ν_{ML} (ca. 100-200 cm^{-1}), symmetric stretch ν_s (ca. 1340 cm^{-1}) and asymmetric stretch ν_{as} 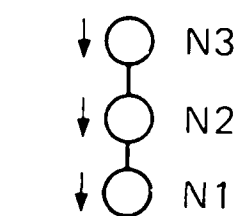(ca.2050 cm^{-1}) to the electrode surface for perpendicular (top) and parallel (bottom) orientations of the azide ion. The azide nitrogens are labelled N1, N2, N3, and the surface silvers schematically represented by the unlabelled circles. The shaded circle represents the top-site, being the only silver atom included in the ab initio calculations.

Figure 2. FT-IRRAS spectra from a Ag electrode in an azide solution in the thin-layer electrochemical cell, showing the potential dependence of the intensity of the 2050 cm^{-1} solution azide v_{as} band. Note the development of a shoulder near 2080 cm^{-1} as the potential is made more anodic. Spectra referenced (by subtraction) to a spectrum of 0.5M NaClO$_4$ solution containing no azide at -0.95V. All potentials measured relative to the Ag/AgCl reference electrode. Electrolyte 30 mM azide in 0.1M NaClO$_4$.

Figure 3. FT-IRRAS spectra of the electrochemical cell. Same data as shown in Figure 2 except all spectra are referenced to (subtracted) the azide spectrum taken at −0.95V. All potentials measured relative to the Ag/AgCl reference electrode. Electrolyte 30 mM azide in 0.1M NaClO$_4$.

Figure 4. Dependence of the surface azide peak vibrational frequency (cm^{-1}) on electrode potential. All potentials measured relative to the Ag/AgCl reference electrode.

FIGURE CAPTIONS

Figure 1. Schematic diagram showing the relation of metal-ligand v_{ML} (ca. 100-200 cm^{-1}), symmetric stretch v_s (ca. 1340 cm^{-1}) and asymmetric stretch v_{as} (ca.2050 cm^{-1}) to the electrode surface for perpendicular (top) and parallel (bottom) orientations of the azide ion. The azide nitrogens are labelled N1, N2, N3, and the surface silvers schematically represented by the unlabelled circles. The shaded circle represents the top-site, being the only silver atom included in the ab initio calculations.

Figure 2. FT-IRRAS spectra from a Ag electrode in an azide solution in the thin-layer electrochemical cell, showing the potential dependence of the intensity of the 2050 cm^{-1} solution azide v_{as} band. Note the development of a shoulder near 2080 cm^{-1} as the potential is made more anodic. Spectra referenced (by subtraction) to a spectrum of 0.5M $NaClO_4$ solution containing no azide at $-0.95V$. All potentials measured relative to the Ag/AgCl reference electrode. Electrolyte 30 mM azide in 0.1M $NaClO_4$.

Figure 3. FT-IRRAS spectra of the electrochemical cell. Same data as shown in Figure 2 except all spectra are referenced to (subtracted) the azide spectrum taken at $-0.95V$. All potentials measured relative to the Ag/AgCl reference electrode. Electrolyte 30 mM azide in 0.1M $NaClO_4$.
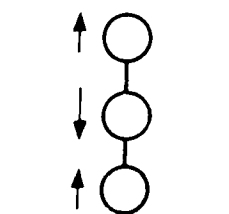
Figure 4. Dependence of the surface azide peak vibrational frequency (cm^{-1}) on electrode potential. All potentials measured relative to the Ag/AgCl reference electrode.
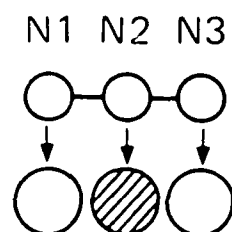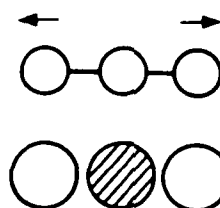
ν_{ML} ν_s ν_{as}
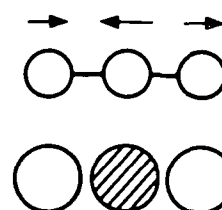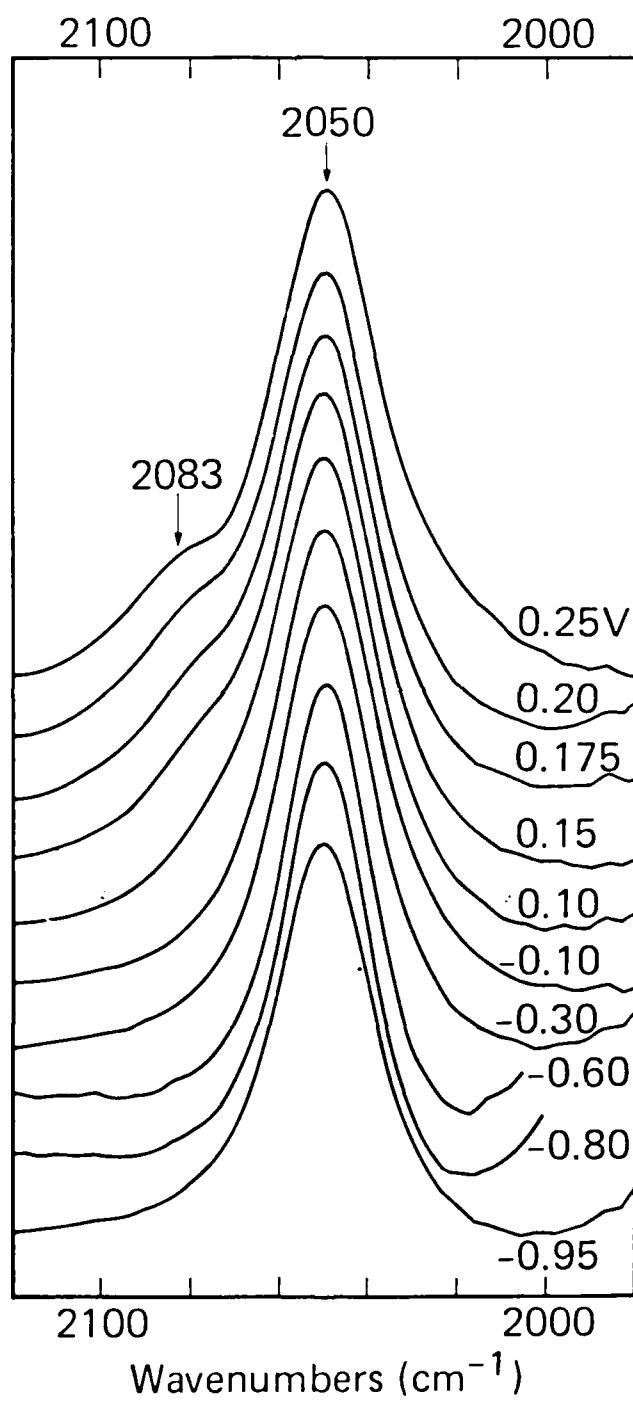
ν_{ML} ν_s ν_{as}

Wavenumbers (cm^{-1})

Wavenumbers (cm^{-1})

2090

2070

ν_{as}/cm^{-1}

2050

0.1　　　0.2　　　0.3

Electrode Potential

END

DATE
FILMD

3-88
DTIC